scientific reports

Check for updates

OPEN

Platelet aggregation elicits FasL expression and hepatocyte apoptosis in sinusoidal obstruction syndrome

Yuri Higashi[1], Seiichi Munesue[2], Masakazu Saeki[1], Ai Harashima[2], Kumi Kimura[2], Yu Oshima[2], Ryohei Takei[1], Satoshi Takada[1], Shinichi Nakanuma[1], Isamu Makino[1], Tetsuo Ohta[1], Shintaro Yagi[1], Hidehiro Tajima[3] & Yasuhiko Yamamoto[2]✉

Sinusoidal obstruction syndrome (SOS) is a fatal liver condition resulting from sinusoidal endothelial cell injury and hepatocyte death, following liver or hematopoietic stem cell transplantation as well as chemotherapy. We showed evidence of platelet displacement and aggregation within the space of Disse in SOS. However, the relationship between platelets and hepatocyte death remains unclear. Using a mouse SOS model by intraperitoneal monocrotaline (270 mg/kg; a pyrrolizidine alkaloide plant toxin) administration, we observed positive stains for terminal deoxynucleotidyl transferase dUTP nick end labeling (TUNEL) and cleaved caspase-3, which are markers for apoptosis, in the liver by immunohistochemistry. At 48 h of the SOS liver, aggregated platelets and hepatocytes around zone 3 were found to express Fas ligand (FasL) and Fas, respectively. Human peripheral blood platelets, when aggregated, could induce expression of FASL on themselves and then lead to apoptosis in co-cultured HepG2 cells. Treatment of recombinant soluble thrombomodulin (rTM), an anticoagulant and vascular endothelium-protective drug, prevented the hepatocyte death in the SOS mice. These findings suggest that the prevention of platelet aggregation is a potential therapeutic intervention against hepatocyte death and severe liver damage in SOS.

Sinusoidal obstruction syndrome (SOS) is a fatal liver injury that occurs after liver transplantation, hematopoietic stem cell transplantation, or chemotherapy[1–4]. The incidences of SOS after liver transplantation and stem cell transplantation are reported to be 0.3–2.3% and 5–60%, respectively[5–8]. The fatality rate of severe SOS exceeds 80%[9]. The liver is composed of small divisions called liver lobules, which consist of a portal triad, linear cords of hepatocytes separated by adjacent sinusoids, and a central vein. The liver lobules are typically subdivided into three metabolic zones: zones 1, 2, and 3[10–12]. Zone 1 hepatocytes encircle portal tracts that are exposed to nutrient- and oxygen-rich blood and engage mainly in glycogen synthesis, gluconeogenesis, protein synthesis, urea synthesis, and β-oxidation of lipids. Zone 3 hepatocytes are located around the central veins and are responsible for glycolysis, lipogenesis and biotransformation reactions. Zone 2 hepatocytes are located between zones 1 and 3 and have an intermediate phenotype[13]. Zone 3 is characterized by blood with a low partial pressure of oxygen, rendering it more susceptible to damage induced by hypoxia resulting from impaired blood flow[14]. SOS progresses mainly in the central venous region (zone 3) and exhibits symptoms of portal hypertension, including splenomegaly and thrombocytopenia[15,16]. The pathological features include initial damage to the liver sinusoidal endothelial cells (LSEC) accompanied by red blood cells (RBC), leukocytes, and platelets dissecting the space of Disse in the SOS[17–19]. Damaged LSEC can lead to embolization and obstruction of sinusoidal flow, resulting in portal hypertension and centrilobular hepatocellular injuries, accompanied by elevation of liver enzymes released into the bloodstream[20]. In general, severe ischemia elicits cell necrosis and energy-independent cell death as opposed to apoptosis or programmed cell death.

We reported that platelets underwent aggregation followed by activation in the space of Disse following LSEC injury, leading to hepatocyte death in zone 3 during the development of SOS[19,21–23]. Hepatocyte death

[1]Department of Hepato-Biliary-Pancreatic Surgery and Transplantation/Pediatric Surgery, Kanazawa University Graduate School of Medical Sciences, 13-1 Takara-machi, Kanazawa 920-8641, Japan. [2]Department of Biochemistry and Molecular Vascular Biology, Kanazawa University Graduate School of Medical Sciences, 13-1 Takara-machi, Kanazawa 920-8640, Japan. [3]Department of Gastroenterological Surgery, Dokkyo Medical University Saitama Medical Center, 2-1-50 Minami-Koshigaya, Koshigaya 343-8555, Japan. ✉email: yasuyama@med.kanazawa-u.ac.jp

is presumed to be caused by necrosis rather than apoptosis in SOS[17,18,24]. However, the correlation between activated platelets and hepatocyte death, including both necrosis and apoptosis, in this detrimental context, remains undetermined.

The Fas receptor (Fas, CD95)-Fas ligand (FasL) pathway is an apoptotic pathway. FAS is expressed on the surface of most cell types, including uninjured hepatocytes[25]. However, FasL expression is notably restricted and primarily observed in natural killer cells, activated T cells, and natural killer T (NKT) cells[25–27]. Once FasL binds to Fas, caspase-8/10 and their downstream effectors caspase-3/7 are activated, triggering apoptosis[28–33]. Schleicher et al. reported that activated platelets and their isolated membrane fractions could solely induce apoptosis in a dose-dependent manner in primary murine neuronal cells, human neuroblastoma cells, and mouse embryonic fibroblasts[34]. It has also been reported that platelet membrane proteins lacking FasL decrease the number of apoptotic cells in mice[34]. Inflammatory stimuli such as tumor necrosis factor-alpha (TNF-α) are known to be involved in the progression of SOS. Furthermore, Kupffer cells are hypothesized to generate TNF-α in a mouse model of liver injury induced by lipopolysaccharide/D-galactosamine[35]. Faletti et al. reported that the stimulation of TNF-α led to the activation of NFκB and subsequent elevation of Fas transcription and protein expression on the hepatocyte cell surface[36]. In addition, Zhou et al. reported that TNF-α exerted an influence on the elevation of the expression of CD40, a member of the TNF-receptor superfamily, on the hepatocyte cell surface within mouse acute hepatitis models induced by concanavalin A and the CD154/CD40 ligand (L)-CD40 axis. Consequently, the effect led to an increase in the expression of Fas in hepatocytes[37]. It is reported that activated platelets could release CD40L[38]. Therefore, we hypothesize that the activation and aggregation of platelets, characterized by the presence of FasL expression within the space of Disses, could induce the release of CD40L. This release, in turn, could lead to an elevation in Fas expression on hepatocytes. Subsequently, the interaction between platelet FasL and hepatocyte Fas would lead to a pernicious cycle, culminating in hepatocyte apoptosis within the context of SOS.

This study aims to understand and elucidate the potential involvement of platelets in hepatocyte death during the course of SOS. By uncovering the underlying cellular and molecular mechanisms, the goal is to identify preventive and therapeutic approaches to address this life-threatening clinical condition.

Results

Alterations of SE-1 and CD42b expression in the liver of SOS model mice

As an SOS model, we used an intraperitoneal monocrotaline (MCT) (270 mg/kg; a pyrrolizidine alkaloide plant toxin)-administered mice. We first examined lining patterns of LSEC by immunohistochemistry using an anti-hepatic sinusoidal endothelial cell-specific antibody, SE-1 (Fig. 1a). The SE-1-positive signals in zone 3 were found to be scanty at 48 h after MCT injection, in contrast to the pattern seen in the control at 0 h (Fig. 1a). These

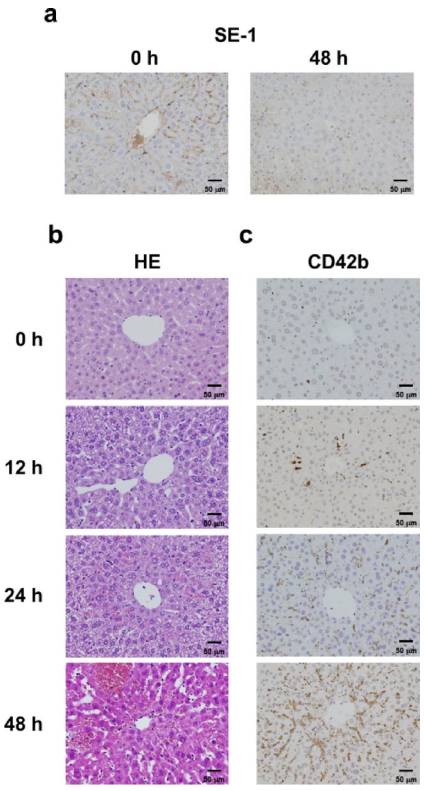

Fig. 1. Immunostaining for SE-1, a LSEC marker, and CD42b, a platelet marker, in the liver of MCT-injected SOS model mice. (**a**) SE-1 staining for LSEC detection at 0 and 48 h after MCT injection. (**b**, **c**) HE (**b**) or CD42b (**c**) staining at 0, 12, 24, and 48 h after MCT injection.

findings are similar to those reported previously[21–23]. Hematoxylin and eosin (HE) staining revealed severe sinusoidal dilatation and substantial hemorrhage at 48 h of MCT administration. Liver damages worsened over time during the observation period (Fig. 1b). We next examined platelet activation and aggregation in SOS-induced liver using an anti-CD42b antibody. Aggregation and clustering of CD42b-positive platelets were observed within the sinusoidal spaces of zone 3 after 48 h of MCT injection (Fig. 1c). In contrast, extremely faint CD42b signals were observed in the control liver at 0 h (Fig. 1c). These findings suggest a possible association between LSECs damages and platelet activation/aggregation in the context of SOS livers.

Apoptosis of hepatocytes in SOS model mice

Next, we examined hepatocyte apoptosis in the livers of SOS mice by immunohistochemistry using an anti-cleaved caspase-3 antibody (Fig. 2a). Positive signals for cleaved caspase-3 were observed in zone 3 hepatocytes at 48 h after MCT injection, but not in the 0 h control (Fig. 2a). Treatment with recombinant human soluble thrombomodulin (rTM), an anticoagulant and vascular endothelium-protective drug, prevented the cleaved caspase-3-positive hepatocyte death in the liver (Fig. 2a). Additionally, TUNEL assay also showed the positive signals in hepatocytes of the SOS model mice (Fig. 2b). These findings indicate that hepatocyte apoptosis in liver zone 3 was induced in the MCT injected SOS model mice and the treatment with rTM could reverse the phenomena.

Expression of Fas and FasL in the liver of SOS model mice

To address the causal factors for the hepatocyte apoptosis in the SOS liver, we examined the involvement of the FasL-Fas system by immunohistochemistry. The results showed that Fas-positive hepatocytes were significantly increased in zone 3 of the liver of MCT-treated SOS model mice at 24 h and 48 h when compared to controls at 0 h (Fig. 3a, b). In contrast, FasL expression was not detectable in hepatocytes, even at 48 h (Fig. 4a). Significant increase of FasL expression was seen in the sinusoids of the liver of SOS model mice (Fig. 4b, d). rTM treatment significantly reduced FasL expression (Fig. 4c, d). CD42b-positive platelets were observed around Zone 3, some extent of which expressed the FasL (Fig. 4e). These findings provide our hypothesis that FasL would appear in activated and aggregated platelets.

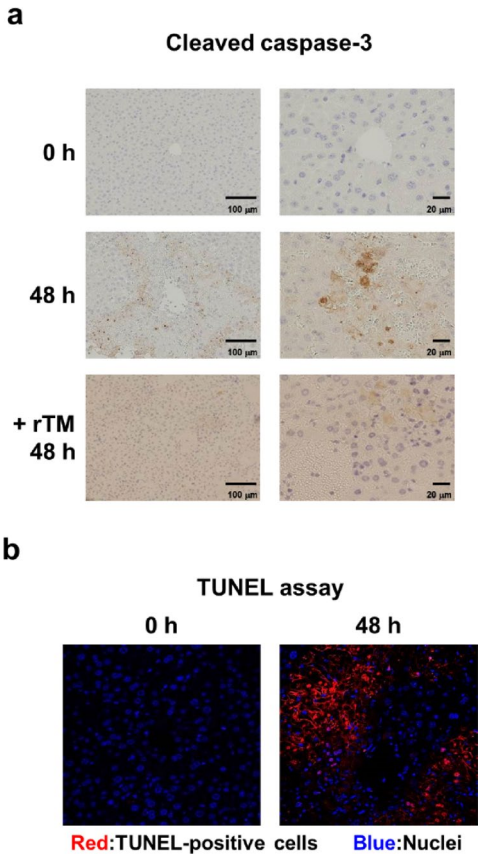

Fig. 2. Immunostaining for cleaved caspase-3 and TUNEL assay in the liver of MCT-injected SOS model mice. (**a**) Cleaved caspase-3 staining at 0 and 48 h after MCT injection. +rTM, pretreatment of recombinant human soluble thrombomodulin (4 mg/kg). (**b**) TUNEL assay at 0 and 48 h after MCT injection.

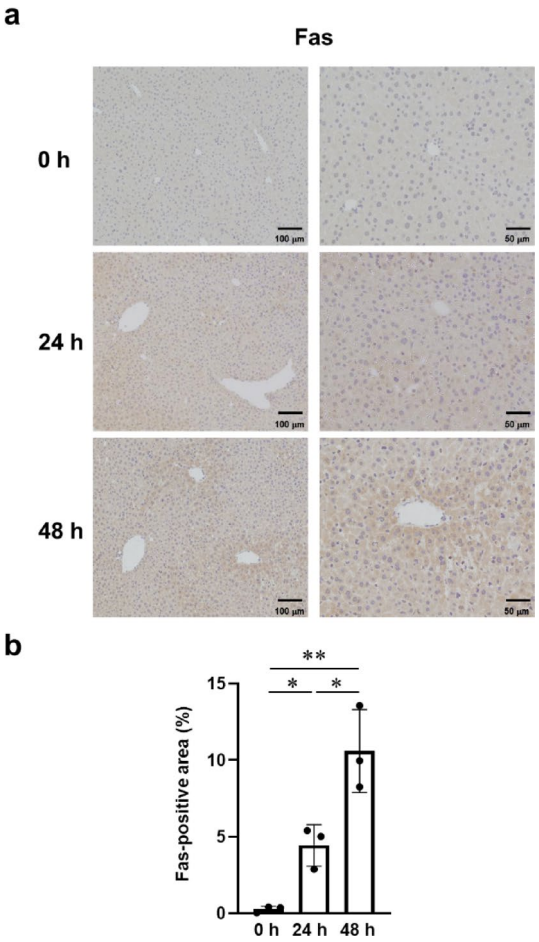

Fig. 3. (**a**) Immunostaining for Fas in the liver at 0, 24 and 48 h after MCT injection. (**b**) The quantitative evaluation of the Fas-positive area. Data are expressed as mean ± SE ($n = 3$). **, $p < 0.01$. *, $p < 0.05$.

FasL-Fas system and hepatocyte apoptosis in SOS model mice

To explore FasL expression on activated platelet surface, we performed western blotting using platelet derived from the liver vasculature of 48 h SOS model mice (Fig. 5a, Supplementary Fig. S1 and 2). FasL protein expression was detectable in platelets derived from the liver vasculature, but not from peripheral blood, of MCT-injected SOS model mice (Fig. 5a, Supplementary Fig. S1). In addition, FasL was not seen in platelets of non-SOS control mice (Fig. 5a, Supplementary Fig. S1).

Next, we addressed whether FasL expression could also be inducible in human platelets. We isolated platelets of peripheral blood from healthy human volunteers and then activated them for further studies. CD62P-positive platelets were defined as activated and coagulated platelets (Fig. 5b, Supplementary Fig. S2). Immunofluorescent study revealed significant increase of FasL expression in the platelets (Fig. 5b, c). FasL signals were not detected in non-activated and unaggregated platelets, which lacked CD62P expression (Fig. 5b). To rule out the presence of non-specific signals from activated and coagulated platelets, we confirmed no signals using the control IgG staining (Fig. 5b). Furthermore, western blot analyses showed a significant increase of FasL expression in human activated and coagulated platelets (Fig. 5d, e, Supplementary Fig. S3). We next performed quantitative polymerase chain reaction (qPCR) analyses and found that the baseline expression level of *FasL* mRNA in non-aggregated platelets was detectable and the level was similar to that in colon adenocarcinoma colon-2 (CACO-2) cells, a colorectal cancer cell line. Peripheral blood mononuclear cells (PBMC) were used as a positive control for *FasL* mRNA expression (Fig. 5f, Supplementary Table S1). We found that *FasL* mRNA was not upregulated in activated and coagulated platelets (Fig. 5f, Supplementary Table S1), thus suggesting that the FasL induction would be controlled at the translational level in response to platelet activation.

Finally, we performed a functional study using a co-culture of HepG2 cells with or without isolated and activated human platelets (Fig. 6, Supplementary Fig. S2). Immunofluorescent analysis showed caspase-3-positive apoptotic HepG2 cells after 2 h of incubation with activated and coagulated platelets, which were positive for CD62P (Fig. 6a, b). After 24 h of co-culture, robust signals of cleaved caspase-3 were observed in HepG2 cells (Fig. 6c), which were significantly suppressed by the treatment of Kp7-6, a Fas/FasL antagonist (Fig. 6d, e). We also performed co-culture experiments using primary mouse hepatocytes and aggregated mouse platelets. The obtained data were compatible with the findings seen in HepG2 cells (Fig. 6f-j). In addition,

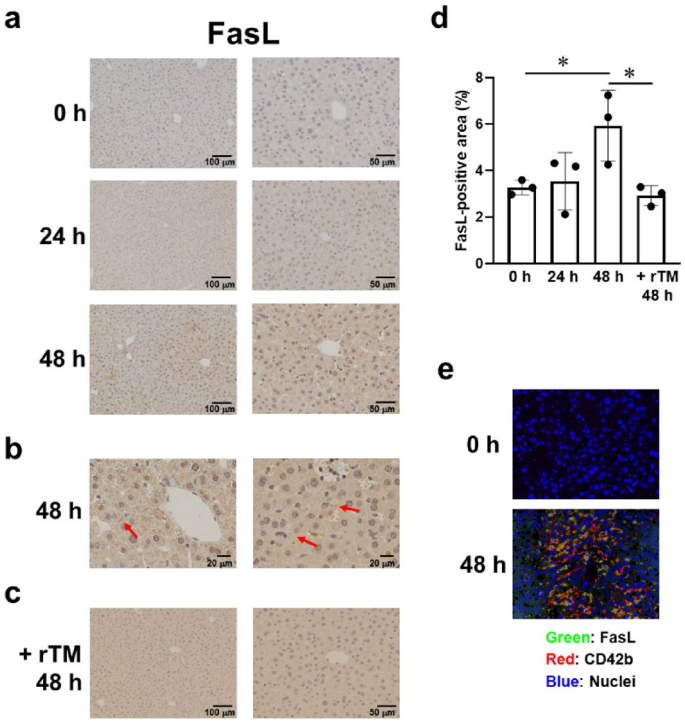

Fig. 4. Immunostaining for FasL in the liver of MCT-injected SOS model mice. (**a**) FasL staining at 0, 24 and 48 h after MCT injection. (**b**) Higher magnification images at 48 h after MCT injection. Red arrows indicate positive stain. (**c**) FasL staining at 48 h after MCT injection in combination with pretreatment of recombinant human soluble thrombomodulin (4 mg/kg). (**d**) The quantitative evaluation of the FasL-positive area. Data are expressed as mean ± SE ($n = 3$). *, $p < 0.05$. (**e**) Immunofluorescent staining for FasL and CD42b.

confocal microscopic analysis revealed the co-localization of FASL and FAS in activated platelets and HepG2 cells, respectively (Supplementary Fig. S4).

Discussion

In pathological processes of SOS, we found that in liver zone 3, (1) LSEC were damaged and CD42b-positive platelets were aggregated (Fig. 1); (2) cleaved caspase-3 and TUNEL-positive apoptosis in hepatocytes were observed (Fig. 2); and (3) FasL appearance on the activated and aggregated platelets led to apoptosis in hepatocytes with Fas expression (Figs. 3, 4, 5 and 6). In addition, treatment with rTM inhibited FasL expression in platelets and hepatocyte apoptosis in the SOS model (Figs. 2 and 4). We also demonstrated platelet FASL-induced apoptosis in FAS-expressing HepG2 cells using a cell culture assay and the phenomenon was reproducible in primary mouse hepatocytes in culture (Fig. 6).

Previous reports have shown that platelet aggregation within Disse's space, in conjunction with damaged sinusoidal endothelial cells, can induce hepatocyte apoptosis in the context of the MCT-treated SOS rat model. This phenomenon was substantiated through techniques such as immunohistochemistry and electron microscopy[21]. Systemic neoadjuvant chemotherapy, e.g. oxaliplatin-based chemotherapy, is clinically used before conversion surgery as a treatment for colorectal cancer patients with liver metastasis. However, oxaliplatin is also known to occasionally cause SOS with platelet aggregation in the space of Disse in zone 3[15]. It has been reported that extravasated platelet aggregates in zone 3 of allograft tissue are associated with liver damages caused by SOS during liver transplantation[19]. Considering these scenarios, antiplatelet therapy is thus one of the potential strategies for mitigating SOS. Miyata et al.. suggested that cilostazol, a potent antiplatelet cyclic nucleotide phosphodiesterase type 3 inhibitor, protects against the development of SOS in a rat model[22]. In addition, human soluble thrombomodulin (rTM) exhibits a prophylactic effect against SOS, attributed to its capacity to safeguard liver sinusoidal endothelial cells in SOS model mice[23]. Defibrotide is an endothelial cell protector and stabilizer that restores thrombofibrinolytic balance, which promotes anti-inflammatory pathways, and decreases the expression of adhesion molecules[39]. Clinical studies and real-world evidence support the efficacy and safety of defibrotide in the treatment of SOS after hematopoietic stem cell transplantation[40–43]. Since platelet aggregation could exacerbate SOS pathologies, antiplatelet therapy drugs (such as aspirin, clopidogrel, cilostazole, and beraprost sodium) would be potential treatment strategies for SOS[44,45].

It is also crucial to understand how apoptosis occurs via the interaction between FasL and Fas in platelets and hepatocytes, respectively, which may be involved in SOS pathogenesis (Fig. 7). Yang et al. reported that Kupffer cells could be involved in the production of TNF-α during liver injury by using a lipopolysaccharide/D-galactosamine-induced SOS mouse model[35]. Faletti et al. reported that TNF-α could activate NFκB, amplify Fas transcription, and then induce the expression of Fas in hepatocytes[36]. In addition, Zhou et al. reported

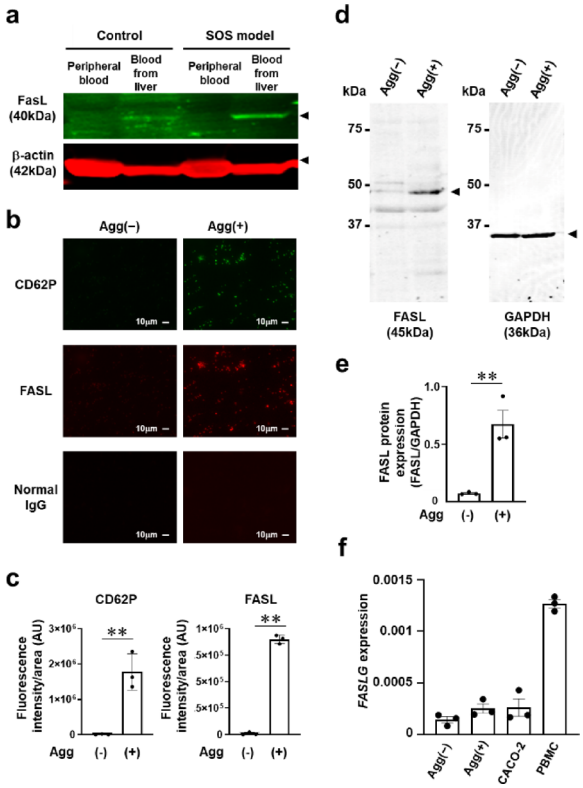

Fig. 5. FasL appearance in activated and aggregated platelets. (**a**) Western blotting for mouse FasL protein in platelets isolated from the peripheral blood and the liver of MCT-injected SOS model mice (SOS model) or non-injected controls (Control). (**b**) Immunofluorescent study for the detection of CD62P and FasL using human platelets with or without their activation and coagulation [Agg(+) or Agg(-), respectively]. Normal IgG used as a negative control. (**c**) The quantitative data of CD62P and FasL fluorescence intensity. Data are expressed as mean ± SE ($n = 3$). **, $p < 0.01$. (**d**) Western blotting for human FasL protein in platelets with or without their activation and coagulation [Agg(+) or Agg(-), respectively]. (**e**) The quantitative data of the band intensity of FASL and GAPDH. Data are expressed as mean ± SE ($n = 3$). **, $p < 0.01$. (**f**) qPCR analyses for FasL mRNA in human platelets with or without their activation and coagulation [Agg(+) or Agg(-), respectively]. CACO-2 cells, colorectal cancer cell line. PBMC, peripheral blood mononuclear cells as a positive control.

that stimulation of TNF-α increased the expression of CD40 on the surface of hepatocytes by utilizing an acute hepatitis mouse model with concanavalin A as well as primary cultured mouse liver cells[37]. Subsequently, stimulation with CD40L increases the expression of Fas in hepatocytes[37]. Activated platelets are recognized for their expression of CD40L, and our study support the evidence that activated platelets in SOS induced CD40L, leading to the expression of Fas on the surface of hepatocytes. The series of steps involved in the expression of FAS in hepatocytes is compatible with our current findings.

Next, we discuss the appearance of FasL in activated and aggregated platelets, as shown in Figs. 4 and 5. Our findings align with a previous report by Schleicher et al. who observed the membrane-bound FasL on activated platelets caused neuronal apoptosis in ischemic stroke[34]. In general, platelets are capable of activating anti-apoptotic pathways, thereby altering the balance between cell survival and tissue repair[46]. Platelet-derived microparticles can induce Akt phosphorylation in neural stem cells and endothelial cells, leading to cell proliferation, survival, and differentiation[47,48]. Moreover, platelets are known to secrete mediators with anti-apoptotic activity upon activation, such as hepatocyte growth factor (HGF), stromal cell-derived factor (SDF-1), serotonin, adenosine diphosphate, and sphingosine-1-phosphate, all of which promote survival signals[49–53]. On the other hand, a candidate for the platelet-mediated regulation of cell death is high-mobility group box 1 (HMGB1), a nuclear protein passively released by necrotic cells during tissue injury or actively secreted by innate immune cells as a distress signal that activates immune responses[54,55]. Platelets contain endogenous HMGB1, which is exported to the cell surface upon activation[56]. Regarding FasL in platelets, unstimulated and inactivated platelets lack FasL; this strongly suggests renewed translation and synthesis of the FasL protein in the platelet cytoplasm upon activation. We reviewed the literature and found several reports in this context. Anucleated platelets regulate interleukin (IL)-1β synthesis by splicing pre-mRNAs[57]. Thrombin, lipopolysaccharide, or clustering of Fc alpha receptor 1(FcαR1) could induce IL-1β pre-mRNA splicing and subsequent translation of IL-1β protein in platelets[57–60]. Tissue factor (TF) is a critical procoagulant protein involved in the initiation and propagation of clots[61]. TF pre-mRNA splicing and protein production were also observed in the activated platelets of humans[59,62]. In this study, we discovered the appearance of FasL in platelets, which occurs through translational control upon stimulation in the liver of a mouse model of SOS.

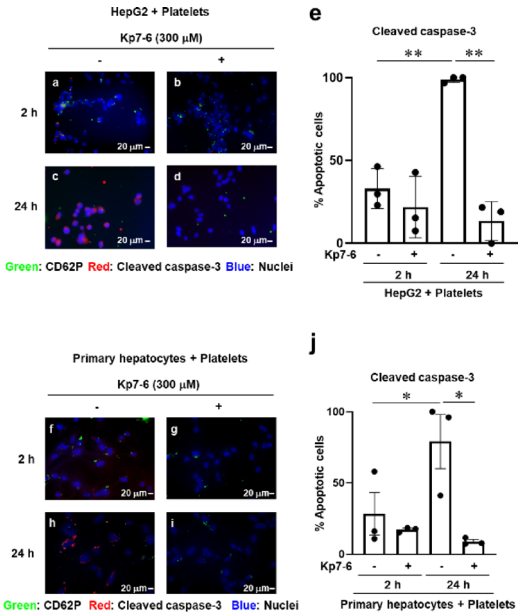

Fig. 6. Immunofluorescent study for the detection of cleaved caspase-3 in HepG2 cells (**a**-**d**) or primary mouse hepatocytes (**f**-**i**) at 2–24 h after co-incubation of activated and coagulated human or mouse platelets with or without the treatment of 300 μM of Kp7-6, a Fas/FasL antagonist. (**e** and **j**) The quantitative data of cleaved caspase-3 fluorescence intensity. Data are expressed as mean ± SE ($n = 3$). **, $p < 0.01$.

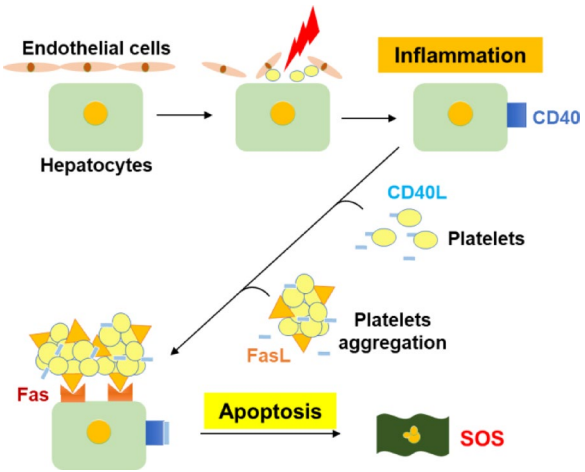

Fig. 7. A proposed model of hepatocyte apoptosis after the interaction between FasL on activated and coagulated platelets and Fas-expressed hepatocytes in the pathogenesis of SOS.

In the future, by identifying how and when platelets generate FasL, we may be able to understand the role of platelets not only in SOS but also across a spectrum of liver diseases, including nonalcoholic steatohepatitis. It has also been reported that Kupffer cells express FasL[63] and that hepatocytes themselves express FasL upon TNF-α and CD 40 L stimulation[64]. Investigating the potential contribution of Kupffer cells to the induction of hepatocyte apoptosis and elucidating whether hepatocytes can initiate the Fas-FasL pathway interaction with them holds the promise of enhancing our comprehension of the underlying mechanisms driving the pathogenesis of SOS.

In conclusion, this study has revealed that Fas expression within hepatocytes could be enhanced around zone 3. This tandem occurrence implies the potential initiation of hepatocyte apoptosis via the Fas-FasL pathway. Thus, we propose that antiplatelet therapy could stand as a potential therapeutic intervention to counter hepatocyte death and mitigate severe liver damage in patients with SOS.

Methods

Ethical declaration

The experimental protocols with mice were approved by the Committee on Animal Research and Resources of Kanazawa University (AP-194058). All trial protocols were achieved in concurrence with the Standard Guidelines for the Care and Use of Laboratory Animals and in accordance with ARRIVE guidelines. All ethical considerations and guidelines were followed during the testing period and specimen collection to ensure that animal suffering was effectively minimized.

The study with human complied with the ethical principles set forth in the Helsinki Declaration and Japan's Personal Information Protection Act, and was conducted in accordance with the Ethical Guidelines for Medical Research Involving Human Subjects (Public Notice of Ministry of Education, Culture, Sports, Science and Technology/Ministry of Health, Labor and Welfare). The experimental plan was approved by the ethics committee of Kanazawa University (2018 – 229). Informed consent was obtained from subjects prior to the tests, and the subjects sufficiently understood the content of the testing plan and voluntarily expressed their willingness to participate in the test.

Reagents and methods

Monocrotaline (MCT) was purchased from FUJIFILM Wako Pure Chemical Corporation (Osaka, Japan). To prepare the MCT solution, the powder was dissolved in 1.0 N HCl and then adjusted to pH 7.4 with 0.5 N NaOH. A Fas/FasL antagonist, Kp7-6, was purchased from Merck KGaA (Darmstadt, Germany).

Animals

Female Crl: CD1 mice (six-week-old, 15–25 g) and male C57BL/6J mice (eight–twelve-week-old, 24–27 g) were purchased from Charles River Laboratories (Kanagawa, Japan). The mice were treated under specific pathogen-free conditions and given free access to food and water according to the Guidelines for Proper Conduct of Animal Experiments and Related Activities in Academic Research Institutions of Kanazawa University, in agreement with the guidelines of the Ministry of Education, Culture, Sports, Science, and Technology of Japan. Euthanasia was performed in a humane manner using decapitation under isoflurane anesthesia.

Experimental protocols

MCT (270 mg/mLkg) or PBS was administered to the mice via an intraperitoneal injection after 12 h of fasting. We chose the optimal MCT concentration according to the previous studies[45,65–68]. The mice were sacrificed at 12, 24, and 48 h after the injection. Recombinant human soluble thrombomodulin (rTM, 4 mg/kg; Asahi Kasei Pharma, Tokyo, Japan) was intraperitoneally injected for 1 h before MCT injection. The livers were removed and fixed in a 10% formalin solution. Samples were embedded in paraffin and sectioned. HE staining was performed for all sections, and immunohistochemical staining was performed using the following primary antibodies: anti-CD42b antibody (ab183345, rabbit monoclonal IgG, diluted 1:100; Abcam, Tokyo, Japan), hepatic sinusoidal endothelial cell antibody (SE-1) (NB110-68095, mouse monoclonal IgG2a Kappa, diluted 1:200; Novus Biologicals, Centennial, USA), cleaved caspase-3 (Asp175) antibody(♯9661, rabbit monoclonal IgG, diluted 1:300; Cell Signaling Technology, Tokyo, Japan), anti-Fas antibody (ab82419, rabbit polyclonal IgG, diluted 1:50; Abcam) and Fas ligand antibody (bs-0216R, rabbit polyclonal IgG, diluted 1:200; Bioss Antibodies, Woburn, USA). We performed a TUNEL assay using a TUNEL Assay Kit (ab66110; Abcam) and observed the cells with a confocal laser scanning microscope (LSM5 PASCAL; Carl Zeiss, Germany).

Platelet isolation

Platelet isolation was performed using the method of Aurbach et al.[69]. Approximately 900 µL of mouse blood was collected from the heart and subjected to mixing with 100 µL of anticoagulation buffer (85 mM tri-sodium citrate dehydrate, 71 mM citric acid monohydrate, 111 mM D-glucose, pH 4.5). This was used as the peripheral blood sample. Non-perfused mouse livers were homogenized in anticoagulant buffer. The homogenate was then used as the blood sample containing platelets derived from the liver vasculature. Human blood samples were also collected in the same methods as mice. Human blood was collected and one-ninth of the blood volume of anticoagulation buffer was added to the human blood sample. Each blood sample was centrifuged at 200 × g for 8 min and transferred to a new tube containing 300 µL of washing buffer (140 mM NaCl, 5 mM KCl, 12 mM trisodium citrate, 10 mM D-glucose, 12.5 mM sucrose, pH 6.0). Following this, the samples were centrifuged at 200 g for 6 min, and platelet-rich plasma was transferred into a new tube containing 300 µL of the wash buffer. The sample was then centrifuged at 1,000 × g for 5 min, and the supernatant was discarded. The pellet obtained was suspended in 800 µL of resuspension buffer (140 mM NaCl, 3 mM KCl, 0.5 mM $MgCl_2$, 5 mM $NaHCO_3$, 10 mM D-glucose, 10 mM HEPES, pH 7.4) and the platelets were subsequently incubated for 30 min at 37℃. The previously described protocol was used for human peripheral blood with 10 volumes of solution and samples.

Flow cytometric analysis

The separation efficiency and purity of isolated mouse platelets were evaluated by flow cytometry. We used an anti-CD41 primary antibody (ab33661, rat monoclonal IgG, diluted 1:100; Abcam) and an anti-CD42b primary antibody (ab183345, rabbit monoclonal IgG, diluted 1:100; Abcam) in combination with Alexa Fluor 488-conjugated anti-rat secondary antibody and Alexa Fluor 594-conjugated anti-rabbit secondary antibody (1:250 dilution). Flow cytometric analysis was performed using a BD FACS Aria Fusion system.

Isolated hepatocytes

Primary hepatocytes were isolated from 8–12-week-old male C57BL/6J and cultured as previously described[70]. Briefly, the liver from anesthetized mice was perfused at a rate of 4.5 ml/min for the first 3 min with Hank's

balanced salt solution (HBSS) (Fujifilm Wako Pure Chemical Corp, Osaka, Japan) containing 10 mM Hepes-NaOH (pH 7.4) and then for 17 min with HBSS containing collagenase type I (0.3 mg/ml) (Worthington, Lakewood, NY, USA) and Protease Inhibitor Cocktail Complete-EDTA free (one tablet per 50 ml) (Roche, Basel, Switzerland). Mouse hepatocytes were purified by density gradient centrifugation with Percoll (Sigma, St. Louis, MO, USA), were cultured overnight in Dulbecco's modified eagle's medium (DMEM) containing 10% FBS.

Western blotting

Platelets were collected from the hearts and livers of the control and SOS model mice. The platelet pellet was dissolved in SDS-PAGE sample buffer (1×) and lysates (50 μg of protein) were loaded and resolved in 12.5% gels before being transferred to polyvinylidene fluoride membranes (EMD Millipore, Billerica, MA, USA). The membranes were blocked at room temperature for 1 h with 3% BSA before being incubated with Fas ligand antibody (bs-0216R, rabbit polyclonal IgG, diluted 1:500; Bioss Antibodies) or a mouse anti-β-actin antibody (cat. no. A5441, 1:10,000; Sigma-Aldrich; Merck KGaA) overnight at 4℃. The goat anti-rabbit IRDye 800CW (cat. no. P/N 926-32211) and goat anti-mouse IRDye 680RD (cat. no. P/N 926-68070) were diluted 10,000-fold and used as secondary antibodies. Antigen-antibody complexes were visualized using the Odyssey Infrared Imaging System version 3.0 (LI-COR Biosciences, Lincoln, NE, USA).

We also confirmed FasL expression in human platelets. We collected platelets from the peripheral blood of healthy volunteers and resuspended the pellet in DMEM containing 10% FBS instead of resuspension buffer to aggregate the platelets. Platelets were centrifuged at 1,000 × g for 5 min and diluted in SDS-PAGE sample buffer (×1). The lysates (25 μg of protein) were subjected to sodium dodecyl sulfate-polyacrylamide gel electrophoresis (Bio-Rad, Philadelphia, PA, USA). Proteins were transferred onto polyvinylidene fluoride membranes (Bio-Rad) and blocked with a commercial gradient buffer (EzBlock, Atto) at room temperature for 1 h. The membranes were incubated with Fas Ligand antibody (bs-0216R, rabbit polyclonal IgG, diluted 1:1000; Bioss Antibodies) and anti-β-actin (A5441, mouse monoclonal IgG, diluted 1:5000; Sigma-Aldrich, St.Louis, MO, USA) overnight at 4℃. After incubation with secondary antibodies, anti-rabbit antibody (sc-2357, mouse monoclonal IgG HRP, Santa Cruz Biotechnology, Texas, USA) and anti-mouse antibody (sc-516102, mouse monoclonal IgGκ BP-HRP, Santa Cruz Biotechnology), the antibody-antigen complexes were detected using an ECL Western blotting detection kit (GE Healthcare, Japan) and a LightCapture system (Atto).

Quantitative real-time reverse transcription polymerase chain reaction (qRT-PCR)

We evaluated FasL expression in human platelets, CACO-2 cells, and peripheral blood mononuclear cells (PBMC) using qRT-PCR. We collected platelets from the peripheral blood of healthy volunteers and resuspended the pellet in DMEM containing 10% FBS instead of resuspension buffer to aggregate the platelets. CACO-2 was cultured in MEM containing 20% FBS. PBMC was collected using Lymphoprep (Abbot Diagnostics Technologies AS, Oslo, Norway). Total RNA was isolated using the TRIzol Reagent (Thermo Fisher Scientific, Massachusetts, USA). cDNA was synthesized using 100 ng of total RNA by AffinityScript QPCR cDNA Synthesis Kit (Agilent, California, USA). We performed qPCR using SYBR Green, normalized to β-actin, and used the following primers for FasL: Sense: 5′-GCAGCCCTTCAATTACCCAT-3′ and antisense: 5′-CAGAGGTTGGACAGGGA AGAA-3′.

Immunocytochemistry

Platelets were cultured in LAB-TEK for 24 h in a resuspension buffer for the control and in DMEM containing 10% FBS for stimulation. The platelets were fixed in methanol and acetone (1:1) before blocking. Two primary antibodies were used: an anti-CD62P antibody (ab6632, mouse monoclonal IgG, diluted 1:100; Abcam) and a Fas Ligand antibody (bs-0216R, rabbit polyclonal IgG, diluted 1:100; Bioss Antibodies). The secondary antibodies used included an anti-mouse IgG antibody conjugated with Alexa Fluor® 488 (A11001, goat polyclonal IgG; diluted 1:400; Life Technology, Tokyo, Japan) and an anti-rabbit IgG antibody conjugated with Alexa Fluor® 594 (A11002, goat polyclonal IgG; diluted 1:400; Life technology). The slides were observed under an immunofluorescence microscope (BZ-X700; Keyence, Osaka, Japan).

HepG2 cells or mouse primary hepatocytes were cultured overnight in DMEM containing 10% FBS and co-cultured with human or mouse platelets suspended in DMEM containing 10% FBS for 2–24 h with or without 300 μM of Kp7-6, a Fas/FasL antagonist. Immunocytochemistry was performed with anti-CD62P antibody (ab6632, mouse monoclonal IgG, diluted 1:100; Abcam) and cleaved caspase-3 (Asp175) antibody (♯9661, rabbit monoclonal IgG, diluted 1:100; Cell Signaling Technology). The secondary antibodies used were the same as those described previously. DAPI (4',6-diamidino-2-phenylindole) was used for nuclear staining.

For confocal microscopic analysis, cells were fixed with 4% paraformaldehyde/PBS for 10 min at RT and washed three times with PBS. We used an anti-FASL antibody (ab134401, rabbit polyclonal IgG, diluted 1:200; Abcam) and an anti-FAS antibody (SC-8009, mouse monoclonal IgG, diluted 1:100; Santa Cruz Biotechnology) in combination with the secondary antibodies of an anti-rabbit IgG antibody conjugated with Alexa Fluor® 594 (A11002, goat polyclonal IgG; diluted 1:400; Life technology) and an anti-mouse IgG antibody conjugated with Alexa Fluor® 488 (A11001, goat polyclonal IgG; diluted 1:400; Life Technology, Tokyo, Japan). Hoechst 33,342 was used for nuclear staining. The slides were observed under a confocal laser scanning microscope (LSM 980; Carl Zeiss, Bern, Germany).

Statistical analysis

All results and data are expressed as the mean ± standard error of the mean. Data were analyzed using GraphPad Prism Software (version 10.2.3; GraphPad Prism, USA). *P*-values were calculated using one-way analysis of variance, followed by Tukey's test for multiple comparisons. The significance level was set at $p < 0.05$.

Data availability

The datasets generated and analyzed during the current study are available from the corresponding author upon reasonable request.

Received: 12 September 2024; Accepted: 22 May 2025
Published online: 29 May 2025

References

1. Takamura, H. et al. Severe veno-occulusive disease / sinusoidal obstruction syndrome after deceased-donor and living-donor liver transplantation. *Transpl. Proc.* **46**, 3523–3535 (2014).
2. Sebagh, M. et al. Significance of isolated hepatic veno-occlusive disease / sinusoidal obstruction syndrome after liver transplantation. *Liver Transpl.* **17**, 798–808 (2011).
3. Dignan, F. L. et al. BCSH / BSBMT guideline: diagnosis and management of veno-occlusive disease (sinusoidal obstruction syndrome) following Haematopoietic stem cell transplantation. *Br. J. Haematol.* **163**, 444–457 (2013).
4. Rubbia-Brandt, L. et al. Severe hepatic sinusoidal obstruction associated with oxaliplatin-based chemotherapy in patients with metastatic colorectal cancer. *Ann. Oncol.* **15**, 460–466 (2004).
5. Sebag, M. et al. Significance of isolated hepatic veno-occlusive disease/sinusoidal obstruction syndrome after liver transplantation. *Liver Taranspl.* **17**, 798–808 (2011).
6. Patrono, D. et al. Long-term outcome of veno-occlusive disease after liver transplant: a retrospective single-center experience. Exp. *Clin. Transpl.* **17**, 214–221 (2019).
7. Corbacioglu, S. et al. Stem cell transplantation in children with infantile osteopetrosis is associated with a high incidence of VOD, which could be prevented with defibrotide. *Bone Marrow Transpl.* **38**, 547–553 (2006).
8. Carreras, E. et al. Incidence and outcome of hepatic veno-occlusive disease after blood or marrow transplantation: a prospective cohort study of the European group for blood and marrow transplantation. European group for blood and marrow transplantation. Chronic leukemia working party. *Blood* **92**, 3599–3604 (1998).
9. Coppell, J. A. et al. Hepatic veno-occlusive disease following stem cell transplantation: incidence, clinical course, and outcome. *Biol. Blood Marrow Transpl.* **16**, 157–168 (2010).
10. Kietzmann, T. Metabolic zonation of the liver: the oxygen gradient revisited. *Redox Biol.* **11**, 622–630 (2017).
11. Torre, C., Perret, C. & Colnot, S. Molecular determinants of liver zonation. *Prog Mol. Biol. Transl Sci.* **97**, 127–150 (2010).
12. Rocha, A. S. et al. The angiocrine factor Rspondin3 is a key determinant of liver zonation. *Cell. Rep.* **13**, 1757–1764 (2015).
13. Kurosaki, S. et al. Cell fate analysis of zone 3 hepatocytes in liver injury and tumorigenesis. *JHEP Rep.* **3,** 100315 (2021).
14. Ebert, E. C. Hypoxic liver injury. *Mayo. Clin. Proc.* 81:1232–1236 (2006).
15. Tajima, H. et al. Oxaliplatin-based chemotherapy induces extravasated platelet aggregation in the liver. *Mol. Clin. Oncol.* **3**, 555–558 (2015).
16. Jardim, D. L., Rodrigues, C. A., Novis, Y. A. S., Rocha, V. G. & Hoff, P. M. Oxaliplatin-related thrombocytopenia. *Ann. Oncol.* **23**, 1937–1942 (2012).
17. Liu, F. et al. Clinical characteristics, CT signs, and pathological findings of pyrrolizidine alkaloids-induced sinusoidal obstructive syndrome: a retrospective study. *BMC Gastroenterol.* **20**, 30 (2020).
18. Zhuge, Y. et al. Chinese society of gastroenterology committee of hepatobiliary disease. Expert consensus on the clinical management of pyrrolizidine alkaloid-induced hepatic sinusoidal obstruction syndrome. *J. Gastroenterol. Hepatol.* **34**, 634–642 (2019).
19. Nakanuma, S. et al. Extravasated platelet aggregation in liver zone 3 is associated with thrombocytopenia and deterioration of graft function after Living-Donor liver transplant. *Exp. Clin. Transpl.* **13**, 556–562 (2015).
20. Yang, X. Q., Ye, J., Li, X., Li, Q. & Song, Y. H. Pyrrolizidine alkaloids-induced hepatic sinusoidal obstruction syndrome: pathogenesis, clinical manifestations, diagnosis, treatment, and outcomes. *World J. Gastroenterol.* **25**, 3753–3763 (2019).
21. Hirata, M. et al. Extravasated platelet aggregation in the livers of rats with drug induced hepatic sinusoidal obstruction syndrome. *Mol. Med. Rep.* **15**, 3147–3152 (2017).
22. Miyata, T. et al. Phosphodiesterase III inhibitor attenuates rat sinusoidal obstruction syndrome through Inhibition of platelet aggregation in Disse's space. *J. Gastroenterol. Hepatol.* **33**, 950–957 (2018).
23. Kanou, S. et al. Prophylactic effect of Recombinant human soluble thrombomodulin for hepatic sinusoidal obstruction syndrome model mice. *Vivo* **34**, 1037–1045 (2020).
24. Valla, D. C. & Cazals-Hatem, D. Sinusoidal obstruction syndrome. *Clin. Res. Hepatol. Gastroenterol.* **40**, 378–385 (2016).
25. Nagata, S. Apoptosis by death factor. *Cell* **88**, 355–365 (1997).
26. Aggarwal, B. B. Signalling pathways of the TNF superfamily: a double-edged sword. *Nat. Rev. Immunol.* **3**, 745–756 (2003).
27. Nagata, S. Fas ligand-induced apoptosis. *Annu. Rev. Genet.* **33**, 29–55 (1999).
28. Muzio, M. et al. FLICE, a novel FADD-homologous ICE/CED-3-like protease, is recruited to the CD95 (Fas/APO-1) death–inducing signaling complex. *Cell* **85**, 817–827 (1996).
29. Vincenz, C. & Dixit, V. M. Fas-associated death domain protein interleukin-1beta-converting enzyme 2 (FLICE2), an ICE/Ced-3 homologue, is proximally involved in CD95- and p55-mediated death signaling. *J. Biol. Chem.* **272**, 6578–6583 (1997).
30. Fernandes-Alnemri, T. et al. In vitro activation of CPP32 and Mch3 by Mch4, a novel human apoptotic cysteine protease containing two FADD-like domains. *Proc. Natl. Acad. Sci. U S A.* **93**, 7464–7469 (1996).
31. Muzio, M., Salvesen, G. S. & Dixit, V. M. FLICE induced apoptosis in a cell-free system. Cleavage of caspase zymogens. *J. Biol. Chem.* **272**, 2952–2956 (1997).
32. Kischkel, F. C. et al. Death receptor recruitment of endogenous caspase-10 and apoptosis initiation in the absence of caspase-8. *J. Biol. Chem.* **276**, 46639–46646 (2001).
33. Milhas, D. et al. Caspase-10 triggers bid cleavage and caspase cascade activation in FasL-induced apoptosis. *J. Biol. Chem.* **280**, 19836–19842 (2005).
34. Schleicher, R. I. et al. Platelets induce apoptosis via membrane-bound FasL. *Blood* **126**, 1483–1493 (2015).
35. Yang, P. et al. Kupffer-cell-expressed transmembrane TNF-α is a major contributor to lipopolysaccharide and D-galactosamine-induced liver injury. *Cell. Tissue Res.* **363**, 371–383 (2016).
36. Faletti, L. et al. TNF-alpha sensitizes hepatocytes to FasL-induced apoptosis by NFκB-mediated Fas upregulation. *Cell. Death Dis.* **9**, 909 (2018).
37. Zhou, F. et al. CD154-CD40 interactions drive hepatocyte apoptosis in murine fulminant hepatitis. *Hepatology* **42**, 372–380 (2005).
38. André, P., Nannizzi-Alaimo, L., Prasad, S. K. & Phillips, D. R. Platelet-derived CD40L: the switch-hitting player of cardiovascular disease. *Circulation* **106**, 896–899 (2002).
39. Richardson, P. G. et al. The importance of endothelial protection: the emerging role of defibrotide in reversing endothelial injury and its sequelae. *Bone Marrow Transpl.* **56**, 2889–2896 (2021).
40. Richardson, P. G. et al. Phase 3 trial of defibrotide for the treatment of severe veno-occlusive disease and multi-organ failure. *Blood* **127**, 1656–1665 (2016).

41. Kernan, N. A. et al. Final results from a defibrotide treatment-IND study for patients with hepatic veno-occlusive disease/sinusoidal obstruction syndrome. *Br. J. Haematol.* **181**, 816–827 (2018).
42. Corbacioglu, S. et al. Defibrotide for prophylaxis of hepatic veno-occlusive disease in paediatric Haemopoietic stem-cell transplantation: an open-label, phase 3, randomised controlled trial. *Lancet* **379**, 1301–1309 (2012).
43. Mohty, M. et al. Real-world use of defibrotide for veno-occlusive disease/sinusoidal obstruction syndrome: the defifrance registry study. *Bone Marrow Transpl.* **58**, 367–376 (2023).
44. Sugita, H. et al. Cilostazol improves the prognosis after hepatectomy in rats with sinusoidal obstruction syndrome. *J. Gastroenterol. Hepatol.* **39**, 1413–1421 (2024).
45. Nakura, M. et al. Inhibitory effects of Beraprost sodium in murine hepatic sinusoidal obstruction syndrome. *Anticancer Res.* **40**, 5171–5180 (2020).
46. Gawaz, M. & Vogel, S. Platelets in tissue repair: control of apoptosis and interactions with regenerative cells. *Blood* **122** (15), 2550–2554 (2013).
47. Hayon, Y., Dashevsky, O., Shai, E., Varon, D. & Leker, R. R. Platelet microparticles promote neural stem cell proliferation, survival and differentiation. *J. Mol. Neurosci.* **47**, 659–665 (2012).
48. Mause, S. F. et al. Platelet microparticles enhance the vasoregenerative potential of angiogenic early outgrowth cells after vascular injury. *Circulation* **122**, 495–506 (2010).
49. Nakamura, T., Teramoto, H. & Ichihara, A. Purification and characterization of a growth factor from rat platelets for mature parenchymal hepatocytes in primary cultures. *Proc. Natl. Acad. Sci. U S A.* **83**, 6489–6493 (1986).
50. Stellos, K. & Gawaz, M. Platelets and stromal cell-derived factor-1 in progenitor cell recruitment. *Semin Thromb. Hemost.* **33**, 159–164 (2007).
51. Crowley, S. T., Dempsey, E. C., Horwitz, K. B. & Horwitz, L. D. Platelet-induced vascular smooth muscle cell proliferation is modulated by the growth amplification factors serotonin and adenosine diphosphate. *Circulation* **90**, 1908–1918 (1994).
52. Pakala, R., Willerson, J. T. & Benedict, C. R. Mitogenic effect of serotonin on vascular endothelial cells. *Circulation* **90**, 1919–1926 (1994).
53. Hisano, N. et al. Induction and suppression of endothelial cell apoptosis by sphingolipids: a possible in vitro model for cell-cell interactions between platelets and endothelial cells. *Blood* **93**, 4293–4299 (1999).
54. Scaffidi, P., Misteli, T. & Bianchi, M. E. Release of chromatin protein HMGB1 by necrotic cells triggers inflammation. *Nature* **418**, 191–195 (2002).
55. Andersson, U. & Tracey, K. J. HMGB1 is a therapeutic target for sterile inflammation and infection. *Annu. Rev. Immunol.* **29**, 139–162 (2011).
56. Rouhiainen, A., Imai, S., Rauvala, H. & Parkkinen, J. Occurrence of amphoterin (HMG1) as an endogenous protein of human platelets that is exported to the cell surface upon platelet activation. *Thromb. Haemost.* **84**, 1087–1094 (2000).
57. Denis, M. M. et al. Escaping the nuclear confines: signal-dependent pre-mRNA splicing in anucleate platelets. *Cell* **122**, 379–391 (2005).
58. Lindemann, S. et al. Activated platelets mediate inflammatory signaling by regulated Interleukin 1beta synthesis. *J. Cell. Biol.* **154**, 485–490 (2001).
59. Qian, K. et al. Functional expression of IgA receptor FcalphaRI on human platelets. *J. Leukoc. Biol.* **84**, 1492–1500 (2008).
60. Shashkin, P. N., Brown, G. T., Ghosh, A., Marathe, G. K. & McIntyre, T. M. Lipopolysaccharide is a direct agonist for platelet RNA splicing. *J. Immunol.* **181**, 3495–3502 (2008).
61. Mackman, N. Role of tissue factor in hemostasis and thrombosis. *Blood Cells Mol. Dis.* **36**, 104–107 (2006).
62. Panes, O. et al. Human platelets synthesize and express functional tissue factor. *Blood* **109**, 5242–5250 (2007).
63. Sato, A. et al. Involvement of the TNF and FasL produced by CD11b Kupffer cells/macrophages in CCl4-induced acute hepatic injury. *PLoS One* **9**, e92515 (2014)
64. Afford, S. C. et al. CD40 activation induces apoptosis in cultured human hepatocytes via induction of cell surface Fas ligand expression and amplifies Fas-mediated hepatocyte death during allograft rejection. *J. Exp. Med.* **189**, 441–446 (1999).
65. Ikezoe, T. et al. The fifth epidermal growth factor-like region of thrombomodulin exerts cytoprotective function and prevents SOS in a murine model. *Bone Marrow Transpl.* **52**, 73–79 (2017).
66. Takada, S. et al. Soluble thrombomodulin attenuates endothelial cell damage in hepatic sinusoidal obstruction syndrome. *Vivo* **32**, 1409–1417 (2018).
67. Yamazaki, H. et al. Thrombopoietin accumulation in hepatocytes induces a decrease in its serum levels in a sinusoidal obstruction syndrome model. *Mol Med. Rep* **25**, (2022).
68. Saeki, M. et al. Assaying ADAMTS13 activity as a potential prognostic biomarker for sinusoidal obstruction syndrome in mice. *Int. J. Mol. Sci.* **24**, 16328 (2023).
69. Aurbach, K. et al. Blood collection, platelet isolation and measurement of platelet count and size in mice-a practical guide. *Platelets* **30**, 698–707 (2019).
70. Kimura, K. et al. Endoplasmic reticulum stress inhibits STAT3-Dependent suppression of hepatic gluconeogenesis via dephosphorylation and deacetylation. *Diabetes* **61**, 61–73 (2012).

Acknowledgements

We thank Ms. Yasuyo Futakuchi for supporting our work.

Author contributions

Conceptualization, H.T., T.O. and Y.Y.; methodology, Y.H., S.M., M.S., H.A., K.K., Y.O., I.M. and Y.Y.; validation, Y.H., S.N., and S.Y.; formal analysis, Y.H. and S.M.; investigation, Y.H., S.M. and M.S.; resources, S.M., A.H. and H.T.; data curation, Y.H., S.M. and M.S.; writing-original draft preparation, Y.H.; writing-review and editing Y.Y.; visualization, S.N.; supervision, H.T. and Y.Y.; project administration, S.Y. All authors have read and agreed to the published version of the manuscript.

Funding

This research was supported in part by Grant-in-Aid for Scientific Research from the Ministry of Education, Culture, Sports, Science and Technology, Japan (grant numbers: 21H02695, 20K09029, and 20K07323).

Declarations

Competing interests

The authors declare no competing interests.

Additional information

Supplementary Information The online version contains supplementary material available at https://doi.org/10.1038/s41598-025-03839-2.

Correspondence and requests for materials should be addressed to Y.Y.

Reprints and permissions information is available at www.nature.com/reprints.

Publisher's note Springer Nature remains neutral with regard to jurisdictional claims in published maps and institutional affiliations.